$Kr^{86}(d,p)Kr^{87}$ Reactions and Comparisons with (d,p) Reactions on Sr^{88}, Zr^{90}, and Mo^{92}†

RICHARD E. SASS, BARUCH ROSNER, AND EDWARD J. SCHNEID
University of Pittsburgh, Pittsburgh, Pennsylvania
(Received 2 December 1964)

Eleven energy levels in Kr^{87} were located by the $Kr^{86}(d,p)Kr^{87}$ reaction. The excitation energies of the levels are ground state, 0.55, 1.52, 2.17, 2.34, 2.57, 2.89, 3.09, 3.31, 3.65, and 3.97 MeV. The orbital-angular-momentum transfer as well as the spectroscopic factors were deduced for the predominant transitions with the aid of distorted-wave Born-approximation calculations. A comparison between the proton spectra obtained by the (d,p) reaction on the Kr^{86}, Sr^{88}, Zr^{90}, and Mo^{92} isotones all of which have a closed shell ($N=50$) of neutrons, but different numbers of proton pairs, is discussed.

INTRODUCTION

THE $Kr^{86}(d,p)Kr^{87}$ reaction is studied in this paper with the purpose of locating the low-lying energy levels of Kr^{87} and assigning orbital angular-momentum values to them. Previously, in a study of the $Kr^{86}(d,p)Kr^{87}$ reaction by Wheeler, Schwartz, and Watson in 1953,[1] the ground state and first excited state were observed. The present work identifies 11 excited states and assigns orbital angular-momentum values to eight levels from the angular distribution.

The $Sr^{88}(d,p)Sr^{89}$ reaction has been studied by Cohen[2] and many energy levels and the cross section for the stripping reaction leading to them were determined. In a recent study of the $Sr^{88}(d,p)Sr^{89}$ reaction, Preston, Sampson, and Martin[3] state that the cross sections for the low-lying strontium levels were found to be more than twice as large as the cross sections for corresponding states of zirconium. This result is unexpected by virtue of the following reasoning.

The cross section for a (d,p) reaction, assuming a direct interaction, may be expressed as

$$\frac{d\sigma}{d\Omega}(d,p)=\frac{2J+1}{2I+1}\sigma_{\text{S.P.}}S, \tag{1}$$

where J is the spin of the state observed in the stripping process; I the spin of the target nucleus; and $\sigma_{\text{S.P.}}$ the single-particle cross section derivable, in principle, from reaction theory, and calculated using distorted-wave Born-approximation (DWBA) methods. The single-particle cross section is primarily a function of the orbital angular-momentum transfer l_n, the scattering angle θ, and the energy Q released in the reaction. S is the spectroscopic factor for the observed level, and expresses the overlap between the initial and final nuclear states.[4] The product of $(2J+1)$ times the sum of the spectroscopic factors for transitions leading to states with a definite value of J is equal to the number of empty spaces in that shell-model state.

Kr^{86}, Sr^{88}, Zr^{90}, and Mo^{92} are the four even-even, stable, single closed shell ($N=50$) isotones. For these nuclei there will be $2J+1$ empty spaces in any subshell of the $50\leq N\leq 82$ neutron shell, so that the spectroscopic factors for the (d,p) reactions should all be equal to unity. The single-particle cross section $\sigma_{\text{S.P.}}$ should also be nearly equal. The optical-model parameters on which the absolute magnitude of the calculated DWBA cross sections depend, are very slowly varying functions of the mass number.[5] Therefore the addition of a single neutron outside a closed shell should yield nearly equal cross sections for the corresponding single-particle states of the four isotones. On the other hand, the location of the single-particle state might change owing to the n-p interaction, as the number of proton pairs is different in these isotones. Therefore, when highly enriched Kr^{86} targets became available, the following investigation was undertaken.

EXPERIMENTAL PROCEDURE

The reactions in this experiment were induced by 15-MeV deuterons from the cyclotron at the University of Pittsburgh. The general experimental methods have been described elsewhere,[6] and the scattering system will be described here only briefly.

The Scattering System

After leaving the cyclotron, the deuteron beam is bent through an angle of 16° by a sector magnet and focused on precision slits that are set at 0.79 mm ($\frac{1}{32}$ in.), corresponding to an energy spread of 20 keV. The beam is then bent through an angle of 40° by another sector magnet, and the image of the slits is focused at the center of the main scattering chamber where the gas cell is mounted (see Fig. 1). The portion of the beam that passes directly through the cell is

† Work performed at the Sarah Mellon Scaife Radiation Laboratory and supported by the National Science Foundation.

[1] G. W. Wheeler, R. B. Schwartz, and W. W. Watson, Phys. Rev. **92**, 121 (1953).
[2] B. L. Cohen, Phys. Rev. **125**, 1358 (1962).
[3] R. L. Preston, M. B. Sampson, and K. J. Martin, Can. J. Phys. **42**, 321 (1964).
[4] B. L. Cohen and R. E. Price, Phys. Rev. **121**, 1441 (1961); S. Yoshida, Nucl. Phys. **38**, 380 (1962).
[5] F. G. Perey, Phys. Rev. **131**, 745 (1963); C. M. Perey and F. G. Perey, *ibid.* **132**, 755 (1963).
[6] B. L. Cohen, J. B. Mead, R. E. Price, K. Quisenberry, and C. Martz, Phys. Rev. **118**, 499 (1960).

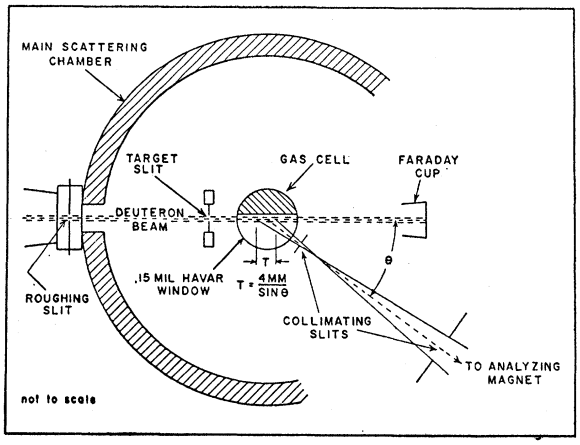

FIG. 1. The scattering-system and gas-cell geometry.

collected in a Faraday cup, and the beam current is electrically integrated. The reaction products then enter a third sector magnet which can be rotated about the scattering chamber to the desired scattering angle. In this experiment, protons from the reaction are bent through an angle of approximately 60° and are focused onto a plate holder along the focal plane of the magnet. A nuclear-track emulsion with a depth of 25 μ is placed in the plate holder. An aluminum absorber is placed over this emulsion. This absorber allows protons to reach the emulsion layer, but is thick enough to stop all other reaction products. After the plates are developed, they are scanned with a microscope, and the tracks are counted and plotted as a function of the distance along the plate.

The Gas Cell

The gas cell is mounted at the center of the scattering chamber. The cell consists of a brass cylinder with a 0.0038-mm (0.15-mil) Havar window that allows the deuteron beam to pass through the cell, and allows the protons from the reaction to be observed at any lab scattering angle from 0 to 180° (see Fig. 1). The window is sealed to the cell by a clamp and O-ring arrangement. The cell can be evacuated through the scattering chamber and can then be sealed off and filled with the target gas. Up to $\frac{1}{2}$ atm of gas may be used safely without rupturing the window. Havar is used for the window rather than Mylar or some other plastic because it is not appreciably affected by the beam currents used in the experiment (about 0.3 to 0.5 μA).

In this experiment the isotopically enriched krypton gas was contained in a small vial which was attached directly to the top of the cell. After the cell was evacuated, the seal on the glass vial was broken and the gas entered the cell. The pressure in the cell, which is proportional to the effective target thickness, was read directly from a pressure gauge attached to the cell structure. After the runs were completed, the krypton gas was recollected by raising a Dewar flask filled with liquid nitrogen around the vial. Because of its low vapor pressure at liquid-nitrogen temperatures, the krypton in the system solidifies in the cold vial. Then the vial can be sealed off and stored for future use.

Directly outside the cell and in line with the magnet entrance port a system of collimating slits was mounted (see Fig. 1). The slits define an active region within the cell and eliminate scattering from, and reactions with, the window. The length of this active region along the beam path is therefore the effective target thickness t. It is approximately 4 mm long at a lab scattering angle of 90°. The target thickness t is then related to the lab scattering angle by the relation

$$t \approx a \csc\theta, \tag{2}$$

where a is the target thickness at 90°.

The Faraday cup does not interfere with the collimator above a lab scattering angle of 11°. To define the solid angle from the gas cell and first slit, the analyzing magnet entrance slit is used as the second slit of the collimating system.

Targets

Krypton

A 10-ml sample of isotopically enriched 95.7% Kr^{86} was used to study the $Kr^{86}(d,p)Kr^{87}$ reaction. As explained earlier, the effective target thickness of a gas target is dependent upon the scattering angle [Eq. (2)]. Besides this, the effective thickness is also a function of the gas pressure. Because of the small sample size, the error in the pressure reading was estimated to be 5%; the error in the length of the active region in the chamber defined by the collimating system was estimated to be around 10%. For this experiment the effective Kr^{86} target thickness as a function of the lab scattering angle was about 0.181 $\csc\theta$ mg/cm^2.

Strontium

The strontium and zirconium targets were both metallic foils. The preparation of the strontium target presented a problem because pure strontium metal oxidizes very rapidly in air, and the metal is usually stored under oil. However, since the low-lying strong states of the $Sr^{88}(d,p)Sr^{89}$ reaction are each separated by about 1 MeV, a semithick target gave resolution sufficient for the determination of the absolute cross sections of these levels. The target was prepared by rolling a small piece of the metal into a thin foil, keeping the entire rolling apparatus wet with kerosene to minimize oxidation. The thickness was measured in the chamber using a ThC alpha source and a solid-state detector at three places on the target, and the results were averaged.

Substantial oxygen and carbon contamination was present on the strontium, and it was realized that part of the thickness of the strontium target was due to these

surface contaminants. It was assumed that the carbon contamination was from the kerosene, so that the carbon was already present when the target thickness was measured. The oxygen contamination was much larger, and due primarily to surface oxidation of the strontium during its exposure to the air. The target was exposed to the air longer during its rolling and mounting than it was after it had been measured, so it was assumed that most of the oxygen had been accumulated by the target before its measurement. To determine the amount of contaminants on the target, the absolute cross sections for the carbon and oxygen peaks were determined from a Mylar target, and those values were used to determine the effective thickness of the contaminants on the strontium target at the same scattering angle. It was assumed that the contaminants were distributed equally on both sides of the target. The energy loss through the contaminant surfaces was determined and the remaining strontium target thickness was calculated as described previously. Two such calculations were made to determine an upper and a lower limit for the oxygen contamination. Upon assuming that half of the final oxygen was present upon measuring the thickness, a strontium target thickness of 8.20 mg/cm^2 was calculated. If all the oxygen was present during the thickness measurement, a strontium thickness of 6.67 mg/cm^2 results. The final value of the target thickness was 7.3 ± 1.2 mg/cm^2, which corresponds to about 80% of the final oxygen contamination present on the spectrum. The natural abundance of Sr^{88} in the target is 82.6%, so the Sr^{89} levels were easily identified.

Zirconium

The zirconium target was a commercial foil whose thickness was previously measured as 2.37 ± 0.24 mg/cm^2 by weighing. The natural abundance of Zr^{90} is 51.5%, and the low-lying levels were easily identified from the known natural zirconium spectrum.[2]

Oxygen

Two oxygen targets were prepared so that the gas-target geometry could be normalized to the standard solid-target geometry. An oxygen-gas target was made by filling the gas cell with oxygen, and the $O^{16}(d,p)O^{17}$ reaction was observed at $\theta_{lab}=20°$. The effective target thickness was 0.38 ± 0.04 mg/cm^2. A solid-oxygen target was prepared by attaching a piece of 0.019-mm (0.75-mil) Mylar to a target holder, and running the same reaction. The Mylar target ($C_{10}O_4H_8$) was measured by weighing to be 2.76 ± 0.01 mg/cm^2.

Information on the target thickness of all the targets used is summarized in Table I.

TABLE I. Summary of target thicknesses.

Target	Thickness (mg/cm^2)	Isotopic abundance %
Kr^{86}	$(0.18\pm0.02)\csc\theta$	95.65
Sr^{88}	7.3 ± 1.2	82.6
Zr^{90}	2.37 ± 0.24	51.5
O^{16}(gas)	0.38 ± 0.04	99.7
O^{16}(Mylar)	2.76 ± 0.01	33.3

The $Kr^{86}(d,p)Kr^{87}$ Reaction

In order to determine the orbital angular-momentum transfer and the absolute cross sections for the (d,p) reactions leading to the various Kr^{87} levels, the proton spectrum was recorded at 12, 16, 20, 25, 30, 38, and 45 deg. The change in the solid angle of the magnetic spectrometer due to the added collimating slits used with the gas cell, as described above had to be taken into account. By carrying out the $O^{16}(d,p)O^{17}$ reaction using a solid (Mylar) and a gaseous oxygen target, and normalizing the ground-state transition cross section obtained by each method, this geometry factor was determined.

A typical $Kr^{86}(d,p)Kr^{87}$ spectrum at 12° is given in Fig. 2 and the angular distribution of the protons in Fig. 3. The excitation energies of Kr^{87} have a maximum uncertainty of 30 keV at a typical excitation of 2 MeV.

The $Sr^{88}(d,p)Sr^{89}$ and $Zr^{90}(d,p)Zr^{91}$ Reactions

Only the absolute cross sections for the (d,p) reactions leading to the first three excited states in Sr^{89} and Zr^{91} were determined. This was done at the angle where the cross section of a given transition has its maximum value, 20° for $l_n=2$ and 30° for $l_n=0$ transitions. These peaks were read twice to minimize the errors in plate reading. The absolute cross sections of zirconium were uncertain by about 20% while those of strontium and krypton were uncertain by 25%. The source of the errors and the estimate of their magnitude was discussed in Ref. 7.

RESULTS AND DISCUSSION

The experimental results for the $Sr^{88}(d,p)Sr^{89}$ and $Zr^{90}(d,p)Zr^{91}$ reactions are tabulated in Table II and for the $Kr^{86}(d,p)Kr^{87}$ reactions in Table III. These tables

TABLE II. Results of the Sr^{88} (d,p) Sr^{89} and Zr^{90} (d,p) Zr^{91} reactions.

Excitation energy (MeV)	l_n	$(d\sigma/d\omega)_{max}$ (mb/sr)	$(2J+1)S$
Sr^{89}			
0	2	14.0	4.33
1.05	0	5.7	1.79
2.02	2	8.3	1.89
Zr^{91}			
0	2	13.3	4.92
1.23	0	4.3	1.53
2.07	2	6.7	1.82

[7] B. Rosner, Phys. Rev. **136**, B664 (1964).

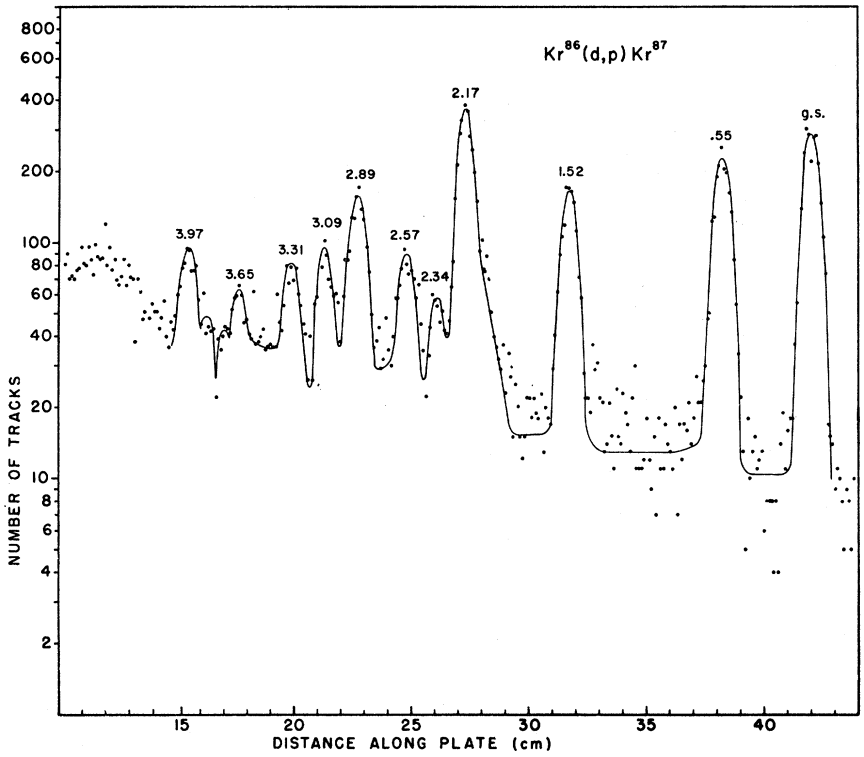

FIG. 2. The $Kr^{86}(d,p)Kr^{87}$ reaction, observation angle $\theta=12°$.

list in successive columns the excitation energies of the observed nuclear levels, the corresponding value of the angular-momentum transfer, the absolute cross sections evaluated at the maximum of the angular distribution, and the spectroscopic factors. The l_n values and the spectroscopic factors were determined with the aid of DWBA calculations. Transitions with cross sections of less than 1 mb/sr were not taken into account because of the presence of 5% of the Kr^{84} isotope in the target which could have accounted for them.

$l_n=2$ Transition

In the three isotones of Kr^{87}, which are Sr^{89}, Zr^{91}, and Mo^{93}, the ground states are $d_{5/2}$ states and the higher states, obtained via $l_n=2$ transitions, were assigned to be $d_{3/2}$ states. Simple shell-model considerations lead

TABLE III. Results of the $Kr^{86}(d,p)Kr^{87}$ reaction.

Excitation energy (MeV)	l_n	$(d\sigma/d\Omega)_{max}$ (mb/sr)	J	S
ground state	2	15.2	$\frac{5}{2}$	0.66
0.55	0	4.7	$\frac{1}{2}$	0.67
1.52	2	5.7	$\frac{3}{2}$	0.31
2.17	2	10.9	$\frac{3}{2}$	0.53
2.34	...	...	...	...
2.57	(2+4)	3.5	$\frac{3}{2}$, $\frac{7}{2}$	...
2.89	2	5.5	$\frac{3}{2}$	0.26
3.09	2	3.4	$\frac{3}{2}$	0.14
3.31	(0+2)	2.2[a]	$\frac{1}{2}$, $\frac{3}{2}$	...
3.65	2	2.4	$\frac{3}{2}$	0.10
3.97	...	...	...	...

[a] Measured at 20°.

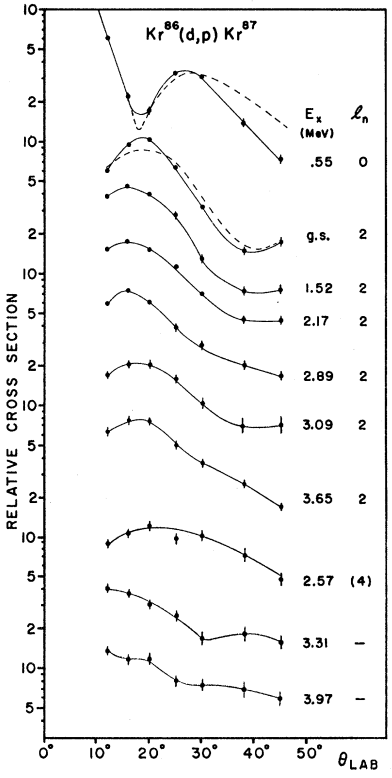

FIG. 3. The angular distribution of protons from the $Kr^{86}(d,p)Kr^{87}$ comparison with DWBA calculations. The solid lines are smooth curves connecting experimental points; the dashed lines are DWBA curves.

one to expect that the $d_{5/2}$ states should appear lower in the spectrum than the $d_{3/2}$ states for these nuclei. Using the shell-model considerations and the similarity of the (d,p) spectra for the four isotones, the ground state of Kr^{87} is most probably a $d_{5/2}$ state and the most of the higher states obtained via $l_n=2$ transitions are expected to be $d_{3/2}$ states.[8,9] With this assignment the spectroscopic factor for the $d_{5/2}$ state is 0.66 whereas for $d_{3/2}$ states it will be 1.35. It is immediately realized that the spectroscopic factor for the $d_{5/2}$ state is lower than the expected value of 1.0 whereas the spectroscopic factor for the $d_{3/2}$ is a little too high. This fact suggests that at least one of the $l_n=2$ excited states is also a $d_{5/2}$ state, in which case the spectroscopic factor would be raised for the $d_{5/2}$ state and lowered for the $d_{3/2}$ state. Unfortunately the $\sigma(d,t)/\sigma(d,p)$ ratio test, successfully applied in many cases,[7,8] could not be applied here as the Kr^{88} isotope is unstable. Neither does the Schiffer effect for $l_n=2$ transitions[10] work in this region at the bombarding energy of 15 MeV as can be seen in the Zr work by Cohen and Chubinsky.[9]

$l_n=0$, 4 Transitions

The only certain $l_n=0$ transition goes to the first excited state at an excitation energy of 0.55 MeV with a cross section corresponding to a spectroscopic factor of 0.67. The angular distribution of the protons leading to the 3.31-MeV state can be resolved into a sum of $l_n=0+2$ transitions, and there may be of course more $l_n=0$ transitions left undetected.

The angular distribution of the protons leading to the 2.57-MeV state peaks certainly at an angle larger than the ones corresponding to $l_n=2$ transitions. An $l_n=4$ assignment for it is confirmed by the location of the similar transitions in Zr^{91} and Mo^{93}. Nevertheless the large cross section for this transition certainly indicates that this state is an $l_n=2+4$ doublet that could not be resolved.

Comparison between the (d,p) Reactions on Kr^{86}, Sr^{88}, Zr^{90}, and Mo^{92}

The four even-even isotones Kr^{86}, Sr^{88}, Zr^{90}, and Mo^{92} all have a closed shell of neutrons ($N=50$), and differ only by the number of proton pairs filling the $28\leq Z\leq 50$ shell. It is therefore expected that the energy spectrum and the transition intensities for the deuteron stripping reactions will be similar, as the captured neutron is populating the empty orbits of the $50\leq N\leq 82$ shell. A schematic representation of the energy levels and the spectroscopic factors for the (d,p) reactions leading to Kr^{86}, Sr^{88}, Zr^{90}, and Mo^{92} is given in Fig. 4. A comparison of the energy difference between the $d_{5/2}$ ground states and the first excited $s_{1/2}$ states reveals that it is the

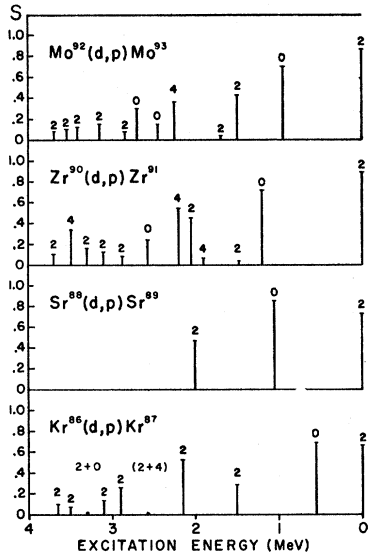

FIG. 4. Schematic representation of the experimental results of the (d,p) reactions with 15-MeV deuterons on Kr^{86}, Sr^{88}, Zr^{90}, and Mo^{92} targets. The numbers on top of the vertical lines indicate the angular-momentum transfer in the transition. The data for the $Mo^{92}(d,p)Mo^{93}$ reaction are from Ref. 8 and those of $Zr^{90}(d,p)Zr^{91}$ from Ref. 9. In S^{88} higher excited states could not be identified because the target was very thick and contained a great deal of oxygen and carbon contamination.

largest for Zr^{91}, somewhat smaller in Sr^{89} and Mo^{93}, and the smallest for Kr^{87}. This same behavior, but to a larger extent, is also seen in the energy interval between the ground states and the second excited states which were assumed to be $d_{3/2}$ states. Despite the shift in energies, the values of the spectroscopic factors for these transitions are rather close to each other. The 25% estimated error in the value of the absolute cross sections prevents us from reaching the conclusion that the spectroscopic factors are really decreasing in magnitude going from Zr^{90} and Sr^{88} towards Mo^{93} and Kr^{87}. The intensity of the stripping reactions leading to levels of excitation between 2 and 4 MeV seems to be similar in three of the cases, whereas for $Sr^{88}(d,p)Sr^{89}$ this could not be determined because of the thick target and the oxygen and carbon contaminations.

These differences and similarities are most likely explained by comparing some features of the nuclear structure of the parent nuclei. In the simple shell-model theory (with no residual forces), Kr^{86} has one proton pair in the $p_{3/2}$ subshell, in Sr^{88} the $p_{3/2}$ subshell is full; Zr^{90} has the closed p-f shell configuration and in Mo^{92} one pair of protons enters into the $g_{9/2}$ subshell. By taking into account the residual interaction between the protons, this simple picture must of course be altered and all the orbits within one shell are assumed to fill more or less simultaneously. The ground state of Zr^{90}, for example, is found to be a $0.75(p_{1/2})^2+0.15(g_{9/2})^2$ mixture,[11] and presumably the ground states of the other

[8] S. A. Hjorth and B. L. Cohen, Phys. Rev. **135**, B920 (1964).
[9] B. L. Cohen and O. V. Chubinsky, Phys. Rev. **131**, 2184 (1963).
[10] L. L. Lee, Jr., and J. P. Schiffer, Phys. Rev. **136**, B405 (1964).
[11] I. Talmi and I. Unna, Nucl. Phys. **19**, 225 (1960).

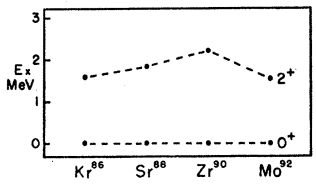

FIG. 5. The excitation energy of the first 2^+ state in Kr^{86}, Sr^{88}, Zr^{90}, and Mo^{92}.

nuclei will have even larger configuration mixing. A possible criterion for comparing the configuration of the ground state of an even-even nucleus to that of a closed-shell configuration is the magnitude of the energy needed for one phonon excitation. The nucleus with a ground state having the most configuration mixing would have the lowest one-phonon excitation energy; conversely, the nucleus with a ground state having a configuration nearest to that of a closed shell would have the highest one-phonon excitation energy. These energies, which are the energy intervals between the 0^+ ground state and the first excited 2^+ state, are shown in Fig. 5. The largest value for this energy is found in Zr^{90} to be 2.182 MeV; a somewhat smaller value of 1.835 is found in Sr^{88}; and the values of 1.54 and 1.57 MeV were found for Mo^{92} and Kr^{86}, respectively.[12,13] It is clearly seen that a correspondence between the one-phonon excitation energy of the parent nucleus and the energy interval between the ground state and the first excited state does exist, whereas no similar correspondence is seen for the transition intensities.

[12] R. Van Lieshout *et al.*, Bull. Am. Phys. Soc. **7**, 342 (1962).
[13] B. Rosner (to be published).

ACKNOWLEDGMENTS

The authors are grateful to Professor B. L. Cohen for his suggestions and encouragement in all phases of this work. They are also indebted to R. H. Fulmer and R. A. Sorenson for helpful discussions, and to R. M. Drisko for his advice in doing the DWBA calculations.

The calculations reported in this article were performed at the University of Pittsburgh computation center which is partially supported by the National Science Foundation under Grant No. G-11309.

APPENDIX: PARAMETERS USED IN DWBA CALCULATIONS

Deuterons

$V=90$ MeV,	$r_0=1.23$ F,	$a=0.64$ F,
$W=48$ MeV,	$r_0'=1.18$ F,	$a'=0.93$ F.

Protons

$V(\mathrm{Zr})=50$ MeV,	$W(\mathrm{Zr})=55$ MeV,	$r_0=r_0'=1.25$ F,
$V(\mathrm{Sr})=51$ MeV,	$W(\mathrm{Sr})=60$ MeV,	$a=0.65$ F,
$V(\mathrm{Kr})=52$ MeV,	$W(\mathrm{Kr})=66$ MeV,	$a'=0.47$ F.

The optical-model potentials used are of the Saxon form with surface derivative absorption.

PHYSICAL REVIEW VOLUME 138, NUMBER 2B 26 APRIL 1965

Effect of an Inelastic Channel on the Position and Width of a Resonance*

PRAN NATH AND Y. N. SRIVASTAVA
Department of Physics, University of California, Riverside, California
(Received 10 December 1964)

The effect of an inelastic channel on the position and width of a resonance is investigated for the case of a two-channel problem using effective-range theory and the uncoupled-phase method. Some estimates are obtained for the shift in the position and reduction in the width of the resonance due to the introduction of the inelastic channel. It is shown that an inelastic channel has, in general, the effect of shifting the resonance maxima towards the first threshold and reducing the asymmetry in width on the high-energy side and the low-energy side of the single-channel resonance. An estimate for the reduction in the asymmetry is also obtained. A two-channel computer experiment is performed to test the quantitative validity of the estimates. Good quantitative agreement of the estimates is obtained with the exact two-channel results.

I. INTRODUCTION

THE effects of an inelastic channel on the resonances or bound states associated with the "old" channel are in general complicated in that they demand solution to the two-coupled-channel problem. Usually calculations made by neglecting a near, closed inelastic channel yield a width of a resonance that is much broader than the observed width. It is generally believed that this width would be significantly reduced if one included the effects due to the nearby inelastic channels. Of course, there is no *a priori* criterion for neglecting a particular channel but it is only after a channel has been properly taken into account that one is sure it has a significant effect. On the other hand, numerical solutions of coupled-channel problems with computers is involved and time consuming and in many situations the effect of an inelastic channel may turn out to be negligible. One would therefore like to have a semi-quantitative estimate of the effect of the inelastic channel before engaging in an involved computer calcu-

* Supported in part by the U. S. Atomic Energy Commission.